Charge-Order Pattern of the Low-Temperature Phase from a Monoclinic Single Domain of NaV_2O_5 Uniquely Determined by Resonant X-Ray Scattering

Kenji Ohwada,[1,*] Yasuhiko Fujii,[2,†] Yuya Katsuki,[2,‡] Jiro Muraoka,[2,§] Hironori Nakao,[3] Youichi Murakami,[3] Hiroshi Sawa,[4] Emi Ninomiya,[4,‖] Masahiko Isobe,[5] and Yutaka Ueda[5]

[1]*Synchrotron Radiation Research Center (SPring-8), Japan Atomic Energy Research Institute, Kohto, Hyogo 679-5148, Japan*
[2]*Neutron Science Laboratory, Institute for Solid State Physics, The University of Tokyo, 106-1, Shirakata, Tokai, Ibaraki 319-1106, Japan*
[3]*Department of Physics, Graduate School of Science, Tohoku University, Sendai, Miyagi 980-8578, Japan*
[4]*Photon Factory, Institute of Materials Structure Science, KEK, Tsukuba, Ibaraki 305-0801, Japan*
[5]*Materials Design and Characterization Laboratories, Institute for Solid State Physics, The University of Tokyo, Kashiwa, Chiba 277-8581, Japan*

(Received 10 August 2004; published 15 March 2005)

The present resonant x-ray scattering has been performed on a monoclinically split single domain of NaV_2O_5. The observation of a critically enhanced contrast between V^{4+} and V^{5+} ions has led us to the unequivocal conclusion of the charge-order pattern of the low-temperature phase of NaV_2O_5 below $T_c = 35$ K. In spite of the possible four types of configuration of the zigzag-type charge-order patterns in the *ab* plane (*A*, *A′*, *B* and *B′*), the stacking sequence along the *c* axis is determined as the *AAA′A′* type by comparison with model calculations.

DOI: 10.1103/PhysRevLett.94.106401 PACS numbers: 71.45.–d, 61.10.Eq, 71.27.+a

Since the discovery of the spin-Peierls-like phase transition of NaV_2O_5 at $T_c = 35$ K [1], its low-temperature structure has been a controversial question. NaV_2O_5 is described well by a system of quarter-filled two-leg spin ladders [2–4], running along the *b* axis of its orthorhombic structure above T_c ($a = 11.3$, $b = 3.65$, $c = 4.8$ Å). All vanadium ions have a nominal valence state of +4.5 ($V^{4.5+}$) at room temperature; one electron is distributed on one V-O-V rung parallel to the *a* axis. At $T_c = 35$ K, NaV_2O_5 undergoes a novel cooperative phase transition associated with its charge disproportionation as $2V^{4.5+} \rightarrow V^{4+}$ (spin state $S = 1/2$) + $V^{5+}(S = 0)$ [5], lattice dimerization as indexed by a $2a \times 2b \times 4c$ supercell [6], and spin-gap formation ($\Delta = 9.8$ meV) [6,7]. The primal analysis of its low-temperature structure based on the space group C_{2v}^{18}-*Fmm*2 [8,9] suggested three different electronic states of V sites, the charge-ordered V^{4+}, V^{5+} and disordered $V^{4.5+}$. However, such a charge distribution is incompatible with experimental results obtained by ^{51}V NMR [5] and resonant x-ray scattering (RXS) measurements [10]. Furthermore, ^{23}Na NMR spectral measurements [11] showed eight independent Na sites, in contrast to only six Na sites led by the space group *Fmm*2. Thus, the low-temperature (LT) structure and its related charge distribution (charge-order pattern) of NaV_2O_5 have long been an interesting topic. In 2002, Sawa *et al.* succeeded in observing Bragg peak splitting below T_c, leading to the fact that the LT phase is *monoclinic* [12,13]. They determined that the LT monoclinic unit cell is constructed as $(a - b) \times 2b \times 4c$ with the space group C_2^3-*A*112, as shown in Fig. 1. By taking into account two types of monoclinically split domains, they obtained a structure completely different from the previously conjectured one with *Fmm*2. The bond valence sum method applied to the new structure results in the V sites being clearly categorized into two groups as charge-ordered V^{4+} and V^{5+} with a zigzag pattern in a ladder as shown in Fig. 1, where a VO_5 pyramid containing V^{4+} is darkly shaded while one for V^{5+} is lightly shaded. The most left two VO_5 pyramid linkages shared with each corner form a ladder running along the *b* axis. Thus, the obtained LT structure is consistent with the previous resonant x-ray [10] and NMR [5,11] data, in striking contrast to the structure previously reported, which included disordered $V^{4.5+}$ sites [8,9].

Figure 1 also shows four types of charge-order pattern in the *ab* plane (called *A*, *A′*, *B*, and *B′*) possibly obtained from the charge ordering upon phase transition. One electron equally shared by two V ions in a rung above T_c is localized at either of two V ions below T_c. In the *A* pattern, for example, V^{4+} is located at each rung within a ladder in a zigzag manner. The *A* and *A′* patterns are related in terms of the translation of $b/2$ along the *b* direction. All ladders have such a zigzag charge order but the spatial relationship between two adjacent ladders results in two types of domain $A(A')$ and $B(B')$ in a single layer, as displayed in Fig. 1. Since the layer-stacking direction along the *c* axis becomes quadruple below T_c, the sequence of these four types of layer is a central issue to be solved to explain all of the observed physical properties, consistently. Recently, Sawa *et al.* [12] have carried out an x-ray diffraction experiment to collect intensity data from a mixed domain sample and to analyze them based on the monoclinic symmetry. They reported that the $ABA'B'$ stacking sequence gives the best fit to the observation. However, there is another candidate for a possible stacking sequence as $AAA'A'$, which also satisfies the space group *A*112. It

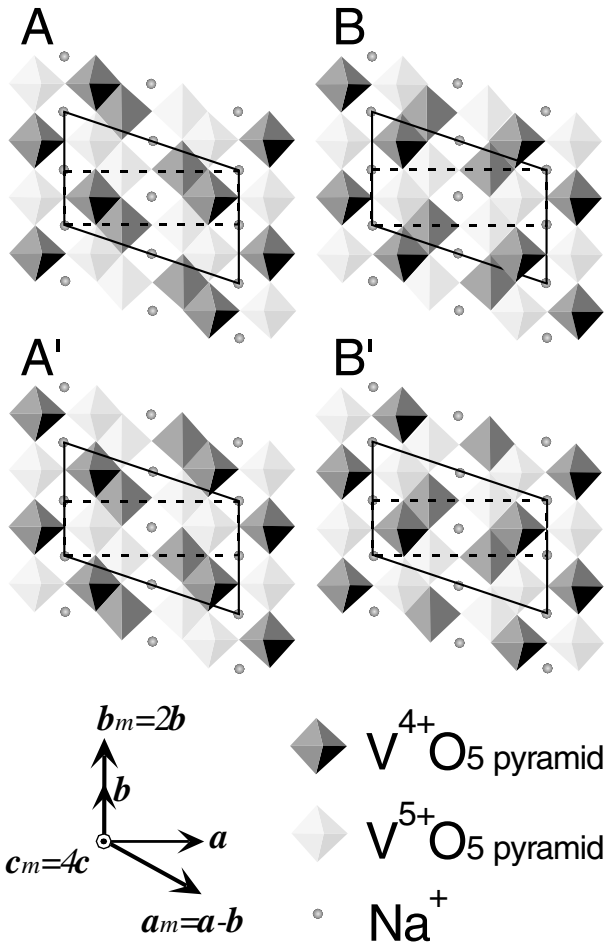

FIG. 1. Zigzag-type charge-order pattern with respect to the configuration of $V^{4+}O_5$ (black) and $V^{5+}O_5$ (white) pyramids lying in the ab plane previously confirmed [12,13]. There are four types of possible in-plane configuration denoted as A, A', B and B'. Dotted and solid lines represent crystallographic unit cells: orthorhombic ($a \times b \times c$) above $T_c = 35$ K and monoclinic ($a_m \times b_m \times c_m$) below T_c.

should be noted that in the domain-averaged intensity-data analysis, the intensity for a combination of the sequences $ABA'B' + BAB'A'$ with an equal domain distribution is found to be the same as that of $AAA'A' + BBB'B'$. This means that a unique structure cannot be obtained unless intensity data are collected from a monoclinic single domain. Such a problem was also pointed out by Grenier *et al.* who conducted a RXS study with domain-averaged data [14]. In spite of such extensive experimental studies for the last eight years, however, the LT structure and charge-order pattern of NaV_2O_5 have not been determined satisfactorily. Once a single domain is available and the charge contrast between V^{4+} and V^{5+} is sufficiently observable near the absorption edge of a V ion, it should be easy to distinguish between the stacking sequences $ABA'B'$ and $AAA'A'$. In this Letter, we have reported the charge-order pattern clearly determined by our RXS experiments using the two types of monoclinically split single domains.

The RXS measurements were performed using synchrotron x rays at beam lines BL-4C and 9C at the Photon Factory of KEK. Incident x rays were monochromatized with a Si(111) double-crystal monochromator. X-ray energy was varied across the V K absorption edge (5.47 keV) which was calibrated with the absorption edge of a V metal foil. A very small single crystal of NaV_2O_5 with dimensions of $58 \times 92 \times 36$ μm^3 ($a \times b \times c$), grown as previously reported [1,15], was mounted on a diamond sample holder [16] using a very small amount of silicone grease so as not to apply any physical stress. Its c axis was set perpendicular to the diamond surface.

Figure 2 shows the peak profiles of the 020 fundamental Bragg reflection taken with $E_i = 5.453$ keV below and above T_c, 7, and 37 K, respectively. In this Letter, the indexing of reflection is based on the orthorhombic lattice above T_c. As previously reported [12], only the b axis in the orthorhombic phase monoclinically moves while both a and c axes retain their directions. Therefore, the peak splitting is clearly associated with such an orthorhombic-to-monoclinic phase transition. The monoclinic peak splitting resulting from two domains (hereafter called domains 1 and 2) starts at T_c with the occurrence of the splitting with decreasing temperature. The splitting angle is almost saturated to $\Delta\omega = 0.07°$ at the lowest temperature which is consistent with previous reports [12,13]. The integrated intensity ratio of domain 1 to domain 2 directly gave a volume ratio of the two domains as approximately 55:45 in the present experiment.

Superlattice reflections also showed such monoclinic splitting so that their energy spectra were measured for the two domains as functions of incident x-ray energy (E_i) across the K absorption edge. The constraint of the present diffraction geometry allowed us to access the following nine superlattice reflections: $\frac{1}{2}\,\frac{1}{2}\,\frac{\bar{1}}{4}$, $\frac{1}{2}\,\frac{3}{2}\,\frac{\bar{1}}{4}$, $\frac{1}{2}\,\frac{3}{2}\,\frac{\bar{3}}{4}$, $\frac{1}{2}\,\frac{5}{2}\,\frac{\bar{1}}{4}$, $\frac{1}{2}\,\frac{5}{2}\,\frac{\bar{3}}{4}$, $\frac{3}{2}\,\frac{3}{2}\,\frac{\bar{1}}{4}$, $\frac{3}{2}\,\frac{3}{2}\,\frac{\bar{3}}{4}$, $\frac{3}{2}\,\frac{5}{2}\,\frac{\bar{1}}{4}$, and $\frac{3}{2}\,\frac{5}{2}\,\frac{\bar{3}}{4}$, where the energy spectra were mea-

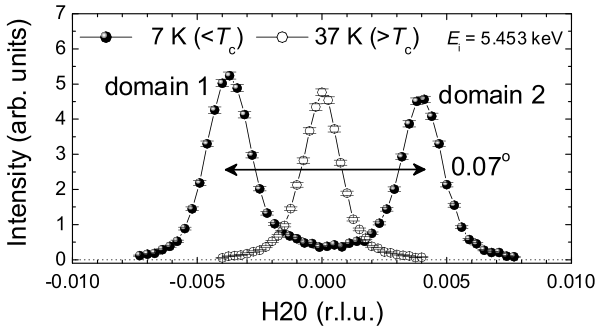

FIG. 2. The observed peak splitting of 020 fundamental Bragg reflection directly evidences the orthorhombic-to-monoclinic phase transition at $T_c = 35$ K. The splitting angle 0.07° is consistent with previous reports [12,13]. The integrated intensity ratio of domain 1 to domain 2 gives a volume ratio of 55:45.

sured for both domains 1 and 2 at 7 K. Figure 3 shows such an energy spectrum of $\frac{3}{2}\,\frac{5}{2}\,\bar{\frac{1}{4}}$ (domain 1) and $\bar{\frac{3}{2}}\,\frac{5}{2}\,\frac{1}{4}$ (domain 2) [17]. Dots in the upper and lower panels represent the experimental data for domains 1 and 2, respectively. One can clearly see markedly different energy spectra between the two domains. The inset in the upper panel of Fig. 3 shows the monoclinic splitting of this superlattice reflection measured at $E_i = 5.47$ keV where the most distinct difference between two domains was observed due to the critically enhanced contrast between V^{4+} and V^{5+} near the absorption edge. A systematic measurement was also made on other eight superlattice reflections.

To compare these observed energy spectra with calculations, we carried out model calculations for the $AAA'A'$ and $ABA'B'$ stacking sequences. The present structure factor calculation was based on the results of the structural analysis performed by Sawa *et al.* [12] and Ninomiya [13]. We used the same anomalous scattering factors $f'$and f'' of V^{4+} and V^{5+} ions as well as the same absorption factor as those used by Nakao *et al.* [10,18] Only two parameters, i.e., a scaling factor and an extinction correction parameter, were adjustable in the calculation. The Lorentz, temperatur, and absorption factors were also taken into account.

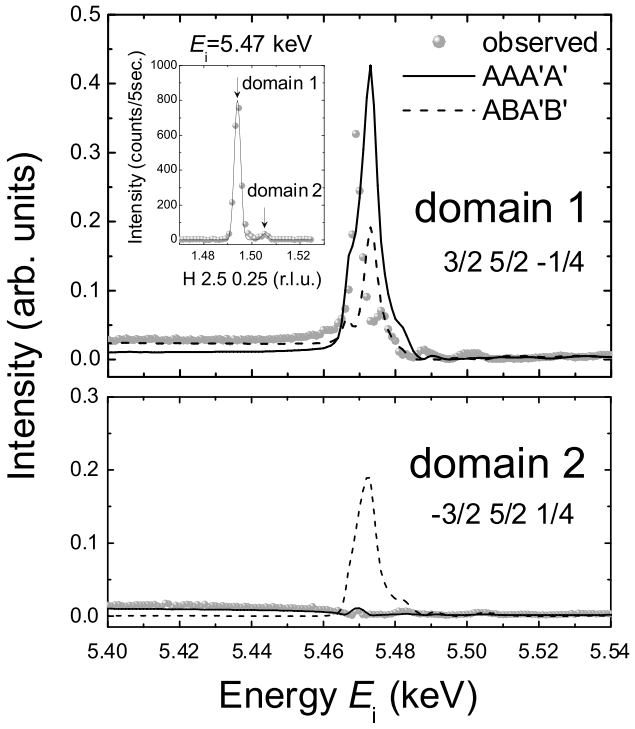

FIG. 3. Observed energy spectra of superlattice reflection $\frac{3}{2}\,\frac{5}{2}\,\bar{\frac{1}{4}}$, from domains 1 (upper) and 2 (lower). The dotted line shows the observed energy spectra while the solid and broken curves represent the calculated intensities based on $AAA'A'$ and $ABA'B'$ sequences, respectively. The inset in the upper panel shows the monoclinic splitting of the superlattice reflections that enable the present RXS to unambiguously determine the charge-order pattern in the LT phase.

The solid and the dotted curves in Fig. 3 represent the calculated results based on the $AAA'A'$ and $ABA'B'$ stacking sequences, respectively. Note that the $AAA'A'$ model reproduces the present observation much better than the $ABA'B'$ model. In particular, the $AAA'A'$ model very well reproduces the critically enhanced intensity on domain 1 and the weak intensity on domain 2. We also calculated the energy spectra of each domain of the other eight superlattice reflections and three fundamental reflections. All the calculated spectra agree with the observation very well and systematically. Figure 4 shows a summary of the observed and calculated intensities at a typical energy $E_i = 5.47$ keV (V K absorption edge) from the nine sets of superlattice reflections. These figures lead us to the unequivocal conclusion that $AAA'A'$ is the right stacking sequence of the charge-order pattern along the c axis in the low-temperature phase of NaV_2O_5. It is essential that such an obtained sequence, $AAA'A'$, simply consists of only two states, A and A'. There is a striking experimental finding regarding NaV_2O_5 that may support the $AAA'A'$ model. Ohwada *et al.* discovered the "devil's staircase" type behavior of the phase diagram of NaV_2O_5 at high pressures and low temperatures [19,20]. The devil's staircase type behavior is originally derived from a well known theoretical ANNNI (axial next nearest neighbor ising) model [21] forming a simple cubic lattice with Ising spins at each corner. Spins lying on the (001) plane interact ferromagnetically with each other, while spins interact

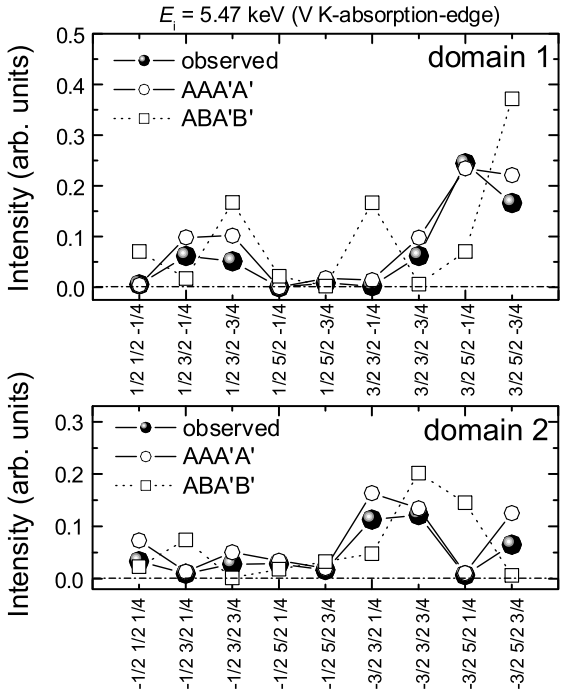

FIG. 4. Observed vs calculated intensities at $E_i = 5.47$ keV (V K absorption edge) of accessible nine sets of superlattice reflections. It is clear that the $AAA'A'$ sequence explains well the experimental results.

ferromagnetically ($J_1 \geq 0$) with the first-nearest neighbor and antiferromagnetically ($J_2 \leq 0$) with the second-nearest neighbor along the [001] (interlayer) direction. Such competitive interactions cause frustration. This model surprisingly produces various types of higher-order commensurate phases with various types of spin modulation along the [001] layer-stacking direction as functions of temperature (T) and the interaction ratio $-J_2/J_1 = \kappa$. For example, the phases with stacking modulations $q = 0, 1/4, 1/5$, and $1/6$ have spin configurations along the [001] direction as $\uparrow\uparrow\uparrow\cdots$ (all up configuration), $\uparrow\uparrow\downarrow\downarrow\cdots$ (up-up-down-down), $\uparrow\uparrow\uparrow\downarrow\downarrow\cdots$ (up-up-up-down-down), and $\uparrow\uparrow\uparrow\downarrow\downarrow\downarrow\cdots$ (up-up-up-down-down-down), respectively. The temperature-pressure phase diagram previously observed in NaV_2O_5 [19,20] very well resembles the T-κ global phase diagram of the ANNNI model. It is quite reasonable to understand that the low-temperature structure with the $AAA'A'$ sequence corresponds to the phase of $q = 1/4$ with an $\uparrow\uparrow\downarrow\downarrow$ configuration of the ANNNI model. The other previously observed phases with wave vectors $q_c = 1/5$, $1/6$, and 0 are also easily understood by the stacking sequences $AAAA'A'\cdots$, $AAAA'A'A'\cdots$, and $AAAA\cdots$, respectively. Thus, the present finding, that is, *the layer stacking sequence is determined unambiguously as* $AAA'A'$, justifies the application of the ANNNI model to NaV_2O_5 under the condition that Ising spins correspond to the charge-order patterns $A(\uparrow)$ and $A'(\downarrow)$. This is a very significant conclusion, because the true character of Ising spins in NaV_2O_5 are clarified experimentally. A highly anisotropic x-ray diffuse scattering previously observed [22,23] suggests a much stronger correlation in the ab plane than in the c axis above T_c. The zigzag-type charge ordering realized below T_c is governed by a strong intersite Coulomb interaction [3] while the $AAA'A'$-type stacking sequence is caused by competitive interactions along the c axis.

In summary, we have succeeded in the unambiguous determination of the charge-order pattern of the low-temperature phase of NaV_2O_5 below $T_c = 35$ K by applying the RXS method to monoclinically split domains. The observed energy spectra of the nine sets of superlattice reflections show an excellent agreement with the calculation based on the $AAA'A'$ model and rule out the $ABA'B'$ model. The experimental fact that a combination of only two states of A and A' form a low-temperature phase offers a clue to understanding the devil's staircase type behavior found in the pressure-temperature phase diagram of NaV_2O_5 with the aid of the ANNNI model. This is the first case that the devil's staircase type phase transition takes place in such a charge-ordered system, where charge-order patterns are regarded as Ising spins.

We would like to thank Dr. Y. Wakabayashi, Dr. Y. Noda, Dr. M. Nishi, Dr. H. Seo, and Dr. H. Fukuyama for stimulating discussions. This work was supported in part by a Grant-In-Aid for Scientific Research from MEXT (Proposal 14740221). Part of this work was supported by the NOP Project under the support from the Special Coordination Funds for Promoting MEXT. The SRX-ray experiments were performed at the Photon Factory with the approval of the Advisory Committee (Proposal 2001G254).

*Electronic address: ohwada@spring8.or.jp
Also at: CREST, Japan Science and Technology Agency, Japan.
†Present address: Neutron Science Research Center, Japan Atomic Energy Reserach Institute, Japan.
‡Present address: Accenture Co., Ltd., Japan.
§Present address: All Nippon Airways Co., Ltd., Japan.
‖Present address: TDK Co., Ltd., Japan.

[1] M. Isobe and Y. Ueda, J. Phys. Soc. Jpn. **65**, 1178 (1996).
[2] H. Smolinski *et al.*, Phys. Rev. Lett. **80**, 5164 (1998).
[3] H. Seo and H. Fukuyama, J. Phys. Soc. Jpn. **67**, 2602 (1998).
[4] K. Tsuda *et al.*, J. Phys. Soc. Jpn. **69**, 1939 (2000).
[5] T. Ohama *et al.*, Phys. Rev. B **59**, 3299 (1999).
[6] Y. Fujii *et al.*, J. Phys. Soc. Jpn. **66**, 326 (1997).
[7] T. Yosihama *et al.*, J. Phys. Soc. Jpn. **67**, 744 (1998).
[8] J. Ludecke *et al.*, Phys. Rev. Lett. **82**, 3633 (1999).
[9] J. L. de Boer *et al.*, Phys. Rev. Lett. **84**, 3962 (2000).
[10] H. Nakao *et al.*, Phys. Rev. Lett. **85**, 4349 (2000).
[11] T. Ohama *et al.*, J. Phys. Soc. Jpn. **69**, 2751 (2000).
[12] H. Sawa *et al.*, J. Phys. Soc. Jpn. **71**, 385 (2002).
[13] E. Ninomiya, Ph. D. thesis, Chiba University, 2003.
[14] S. Grenier *et al.*, Phys. Rev. B **65**, 180101(R) (2002).
[15] M. Isobe *et al.*, J. Cryst. Growth **181**, 314 (1997).
[16] We used a conventional diamond anvil with 600 $\mu m\phi$ culet as the sample holder for the microcrystals.
[17] A set of monoclinic lattices for domain 1 are assigned as ($\boldsymbol{a}_1$, $\boldsymbol{b}_1$, $\boldsymbol{c}_1$, $\gamma_1 \neq 90°$) while another set for domain 2 as ($\boldsymbol{a}_2$, $\boldsymbol{b}_2$, $\boldsymbol{c}_2$, $\gamma_2 \neq 90°$). In the present Letter, the following relations are defined: $\boldsymbol{a}_1 = -\boldsymbol{a}_2$, $\boldsymbol{c}_1 = -\boldsymbol{c}_2$, $\gamma_1 = \gamma_2 \neq 90°$.
[18] For sequential comments and reply of Ref. [10], see J. Garcia *et al.*, Phys. Rev. Lett. **87**, 189701 (2001); J. E. Lorenzo *et al.*, Phys. Rev. Lett. **87**, 189702 (2001); H. Nakao *et al.*, Phys. Rev. Lett. **87**, 189703 (2001).
[19] K. Ohwada *et al.*, Phys. Rev. Lett. **87**, 086402 (2001).
[20] K. Ohwada *et al.*, J. Phys. Soc. Jpn. **69**, 639 (2000).
[21] P. Bak and J. von Boehm, Phys. Rev. B **21**, 5297 (1980); P. Bak, Rep. Prog. Phys. **45**, 587 (1982).
[22] B. D. Gaulin *et al.*, Phys. Rev. Lett. **84**, 3446 (2000).
[23] H. Nakao *et al.*, J. Phys. Chem. Solids **60**, 1101 (1999).